A THEORY OF PULSE PROPAGATION IN ANISOTROPIC ELASTIC SOLIDS

A. N. NORRIS

Department of Mechanics and Materials Science, Rutgers University, Piscataway, NJ 08855-0909, U.S.A.

Received 9 March 1987, Revised 24 June 1987

A theory is described for the propagation of pulses in anisotropic elastic media. The pulse is initially defined by a harmonically modulated Gaussian envelope. As it propagates the pulse remains Gaussian, its spatial form characterized by a complex-valued envelope tensor. The center of the pulse follows the ray path defined by the initial velocity direction of the pulse. Relatively simple expressions are presented for the evolution of the amplitude and phase of the pulse in terms of the wave velocity, the phase slowness and unit displacement vectors. The spreading of the pulse is characterized by a spreading matrix. Explicit equations are given for this matrix in a transversely isotropic material. The rate of spreading can vary considerably, depending upon the direction of propagation. New reflected and transmitted pulses are created when a pulse strikes an interface of material discontinuity. Relations are given for the new envelope tensors in terms of the incident pulse parameters. The theory provides a convenient method to describe the evolution and change of shape of an ultrasonic pulse as it traverses a piecewise homogeneous solid. Numerical simulations are presented for pulses in a strongly anisotropic fiber reinforced composite.

1. Introduction

Many fundamental problems have been solved for wave motion in anisotropic elastic media. A thorough review of plane wave propagation and reflection is given by Musgrave [1]. Solutions for radiation from point forces in full and half-spaces are also known [2, 3]. The more recent monograph of Payton [4] considers transversely isotropic media in detail and also lists more recent references. However, there is a growing need to understand and model the propagation and scattering of finite-sized pulses through anisotropic materials. One area of application, for example, is in ultrasonic inspection of fiber-reinforced composites for purposes of nondestructive evaluation.

The pulses considered here are assumed to be localized in the form of harmonically modulated Gaussian envelopes. The centers of the Gaussian wave packets proagate along the usual rays or characteristic curves. The present theory is an extension of the analysis of Norris [5] on Gaussian wave packets in inhomogeneous acoustic media. The initial ansatz used here is similar for that of time harmonic Gaussian beams; see [6] for a discussion of this in isotropic elastic solids. The Gaussian beam solutions are of infinite extent in the direction of propagation. The present theory includes an extra degree of freedom in that the pulse is of finite length. In the limit as this length becomes infinite, it reduces to time harmonic Gaussian beam theory. It is important to note that the wave packets of this paper and the paper's references [5, 7] are not simply the Fourier transform of a time harmonic Gaussian beam. The distinction is evident from the examples in [5] of a wave packet in an acoustic medium of constant velocity gradient. Some of the cases there cannot be explained by Gaussian beams. Specifically, if the wave packet is initially extended in the direction of propagation, then as the center of the packet follows the curved ray path the bulk of the packet rotates relative to the ray direction. Gaussian beam theory based upon a single beam would predict the solution to be spatially symmetric about the ray path.

Norris [7] considered Gaussian wave packets in inhomogeneous isotropic elastic media and provided explicit formulae for the jump conditions at interfaces. Elastic wave propagation in anisotropic media is complicated by the fact that the wave and phase velocity vectors are distinct for any given wave mode. This leads to the curious result that wavefronts are not orthogonal to the direction of propagation. The general equations of rays and wavefront curvatures in inhomogeneous anisotropic media have been discussed previously, e.g. [8, 9]. The present theory includes these curvature evolution equations as a special case. However, for simplicity only piecewise homogenous media are considered here. The generalization to smoothly varying media is not difficult, but the significance of the results can be obscured by the required amount of excessive notation.

The basic equations are described in Section 2. The general Gaussain wave packet solution is derived and discussed in Section 3. A complete analysis of the reflection/transmission problem for a Gaussian wave packet incident upon an interface is given in Section 4.

2. Eikonal and transport equations

The equations of motion for the displacement field u(x, t) in a homogeneous, anisotropic linearly elastic solid are

$$C_{ijkl}u_{k,jl} - \rho u_{i,n} = 0, \tag{1}$$

where $C_{ijkl} = C_{klij} = C_{jikl}$ is the elastic modulus tensor, ρ the density, and the summation convention on repeated subscripts is assumed. Let [5],

$$u(x,t) = U(x,t) e^{i\omega\phi(x,t)}, \tag{2}$$

$$p = \nabla \phi, \tag{3}$$

then (1) becomes,

$$(i\omega)^{2} [C_{ijkl} p_{j} p_{l} - \rho \phi_{i}^{2} \delta_{ik}] U_{k}$$

$$+ (i\omega) [C_{ijkl} (p_{j} U_{k,l} + p_{l} U_{k,j} + \phi_{,jl} U_{k}) - 2\rho \phi_{i} U_{i,l} - \rho \phi_{il} U_{i}]$$

$$+ [C_{ijkl} U_{k,il} - \rho U_{i,ll}] = 0.$$
(4)

Now consider the asymptotic limit of $\omega \gg 1$. Here ω denotes the center frequency of the solution. Assuming the ansatz

$$U(x,t) = \sum_{n=0}^{\infty} (i\omega)^{-n} U^{(n)}(x,t)$$
 (5)

equation (4) reduces to a sequence of asymptotic equations. The first of these is

$$(C_{iikl} p_i p_l - \rho \phi_l^2 \delta_{ik}) U_k^{(0)} = 0.$$
 (6)

A necessary condition for the existence of a nontrivial solution to (6) is

$$\det(C_{ijkl}p_ip_l - \rho\phi_i^2\delta_{ik}) = 0. \tag{7}$$

In general, there are three independent solutions to (7), of the form [1]

$$\phi_t^2 - f_m^2(p) = 0, \quad m = 1, 2, 3.$$
 (8)

Each function $f_m(p)$ defines a slowness surface. In the case of an isotropic medium, two of the slowness surfaces coalesce and the explicit formulae are

$$f_1(p) = c_L[p \cdot p]^{1/2}, \qquad f_2(p) = c_T[p \cdot p]^{1/2}$$
 (9)

where c_L and c_T are the longitudinal and transverse wave speeds. The three separate identities in (8) are known as the anisotropic eikonal equations.

The next in the sequence of asymptotic equations is

$$[C_{ijkl}(p_j U_{k,i}^{(0)} + p_l U_{k,j}^{(0)} + \phi_{,jl} U_k^{(0)}) - 2\rho \phi_i U_{i,i}^{(0)} - \rho \phi_{it} U_i^{(0)}] + (C_{ijkl} p_j p_l - \rho \phi_i^2 \delta_{ik}) U_k^{(1)} = 0.$$
(10)

Multiply this by $U_i^{(0)}$ and sum over i, using (6), to obtain the anisotropic transport equation

$$C_{ijkl}(p_j U_i^{(0)} U_k^{(0)})_{,l} - \rho(\phi_t U_i^{(0)} U_i^{(0)})_{,l} = 0$$
(11)

3. The Gaussian wave packet solution and evolution equations

3.1. The ray velocity

Consider the following root of the eikonal equation (8),

$$\phi_i + f(\mathbf{p}) = 0, \tag{12}$$

where f(p) is any one of f_1 , f_2 or f_3 . Equation (12) is a first-order partial differential equation in ϕ of the form

$$H(x, t, p, \phi_t, \phi) \equiv \phi_t + f(p) = 0.$$
 (13)

This admits of solutions along characteristic curves in space-time. Let time be the ray parameter along these curves, defined by $x = \bar{x}(t)$, and let an overdot represent the total derivative with respect to t along a ray. Then the Hamilton-Jacobi equations are

$$\dot{t} = \partial H/\partial \phi_t = 1, \qquad \dot{x} = \partial H/\partial p = \partial f(p)/\partial p,$$
 (14a, b)

$$\dot{p} = -\partial H/\partial x = 0, \qquad \dot{\phi}_t = -\partial H/\partial t = 0.$$
 (14c, d)

Equation (14d) implies ϕ_i is constant on a ray. Without loss of generality, this constant can be taken as -1, so that equation (12) for the slowness surface becomes

$$f(p) = 1. ag{15}$$

Equation (14c) show that the slowness vector is constant on a ray, and hence, from (14b), the rays are straight lines. These equations are easily generalized to inhomogeneous media (see [8]).

Define the wave velocity vector c as

$$c = \partial f(p)/\partial p. \tag{16}$$

Thus, c is perpendicular to the slowness surface at p [1]. A more explicit formulation of equation (16) is given in Appendix A. In general (see Appendix A),

$$p \cdot c = 1 \tag{17}$$

512

and

$$p \wedge c \neq 0. \tag{18}$$

Define the wave and phase speeds, c and v, respectively, as

$$c = (c \cdot c)^{1/2}, \qquad v = (p \cdot p)^{-1/2}.$$
 (19)

Therefore, by (17) and (19),

$$c \ge v$$
 (20)

with equality in an isotropic medium, in which case the wave velocity and slowness vectors are parallel $(p \land c = 0)$. Finally, note that the ray equation in a homogeneous medium is

$$\bar{x}(t) = \bar{x}(0) + tc. \tag{21}$$

3.2. Second-order derivatives of the phase

So far, we have derived equations for the evolution along a ray of $\nabla \phi = p$ and ϕ_t , both of which are constant. Next consider the matrix of second-order spatial derivatives,

$$M(t) = \nabla \nabla \phi(\bar{x}(t), t). \tag{22}$$

Along a ray, both

$$\dot{p} = \nabla \phi_t + M\dot{x} = \nabla \phi_t + Mc = 0 \tag{23}$$

and

$$\dot{\phi}_t = \phi_{tt} + c \cdot \nabla \phi_t = 0. \tag{24}$$

It then follows that

$$\nabla \phi_i = -Mc, \tag{25}$$

$$\phi_{tt} = c^{\mathsf{T}} M c. \tag{26}$$

Thus, all the second-order derivatives of the phase can be written in terms of M(t). Let

$$A(t) = \frac{\partial \bar{x}(t)}{\partial \alpha}, \qquad B(t) = \frac{\partial p(t)}{\partial \alpha}, \tag{27}$$

where α is some vector independent of t, e.g., $\alpha = \bar{x}(0)$, the initial ray position. Then,

$$R(t) \equiv M^{-1} = AB^{-1} \tag{28}$$

and

$$\dot{R}(t) = \dot{A}B^{-1} - AB^{-1}\dot{B}B^{-1}. \tag{29}$$

The values of \vec{A} and \vec{B} follow by taking the variation of equations (14b) and (14c) with respect to α . Thus,

$$\dot{A} = NB, \qquad \dot{B} = 0, \tag{30a, b}$$

.

where

$$N_{ij} \equiv \partial^2 f(p)/\partial p_i \partial p_j, \tag{31}$$

Equations (29)-(31) imply

$$\dot{R} = N. \tag{32}$$

Since N is constant, equations (28) and (32) give

$$M(t) = M(0)[I + tNM(0)]^{-1}.$$
(33)

An explicit expression for N of (31) is given in Appendix A (equations (A.12), (A.13) and (A.23)). It is shown in (A.15) and (A.19) that the real-valued matrix N projects onto the plane perpendicular to p, and so one of its eigenvalues is always zero. The other two eigenvalues are related to the principal curvatures of the slowness surface f(p) = 1. Define normal points on the slowness surface as those points at which these two eigenvalues are nonzero. Points that are not normal are inflection points and correspond to cusps on the wave surface. The regions between the cusps define lids on the wave surfaces [2-4]. The areas on the slowness surface associated with the lids are concave. In these regions, the matrix N possesses one or two negative eigenvalues. The two eigenvalues are positive in regions where the slowness surface is convex. The present theory is valid in normal regions of the slowness surface, which thus includes convex and concave parts of the surface. For example, in transversely isotropic materials, points of inflection can only occur on the quasi-transverse (qT) slowness surface, and then only for certain combinations of moduli [4]. These features are illustrated by example below.

We are now able to approximate the phase $\phi(x, t)$ locally in space and time about the ray position $\bar{x}(\tau)$ at time τ . Let

$$\Delta x = x - \bar{x}(\tau), \qquad \Delta t = t - \tau. \tag{34}$$

Then a second-order Taylor series approximation yields, using (3), (22), (25), (26), (34) and $\phi_i = -1$,

$$\phi(x,t) = \phi_0 + (p \cdot \Delta x - \Delta t) + \frac{1}{2} (\Delta x - c \Delta t)^{\mathsf{T}} M(\tau) (\Delta x - c \Delta t), \tag{35}$$

where ϕ_0 is a constant. Since p and c are real vectors, it follows that

$$\operatorname{Im}[\phi(x,t) - \phi(\bar{x}(\tau),\tau)] = \frac{1}{2}(\Delta x - c \,\Delta t)^{\mathrm{T}} \operatorname{Im} M(\tau)(\Delta x - c \,\Delta t), \tag{36}$$

It is clear from (2) and (36) that the solution is in the form of a localized Gaussian wave packet (GWP) if and only if Im M is positive definite. It can be shown, using (30) and the methods of [5, Appendix B] that Im $M(\tau)$ is positive definite for all τ if Im M(0) is positive definite. The other necessary conditions, which are physically obvious, are that M(0) is symmetric and det $A(0) \neq 0$.

Note from (35) that the linear correction to the phases, $(p \cdot \Delta x - \Delta t)$, propagates with the phase velocity $p/|p|^2$. However, the center of the GWP is defined as the point at which the quantity in equation (36) is zero. Therefore, the center propagates with the wave velocity c. This is also apparent from (21). This discrepancy between the two velocities is characteristic of anisotropic media.

3.3. The transport equation

Let g be the unit eigenvector of (6), so that

$$U^{(0)} = U^{(0)}g. (37)$$

Since g is constant, the transport equation (11) reduces to

$$C_{ijkl}g_ig_kp_j\frac{\partial U^{(0)^2}}{\partial x_l}-\rho\phi_t\frac{\partial U^{(0)^2}}{\partial t}+\left[C_{ijkl}\left(g_ig_kM_{jl}+p_j\frac{\partial g_ig_k}{\partial p_m}M_{ml}\right)-\rho M_{ij}c_ic_j\right]U^{(0)^2}=0. \tag{38}$$

Equations (22) and (26) have been used in deriving (38) from (11). Let $\bar{U}^{(0)}(t)$ be the value of $U^{(0)}$ along the ray. Then, since $\phi_t = -1$ and from the identities (A.8) and (A.11), equation (38) reduces to

$$\left(\frac{\partial}{\partial t} + c \cdot \nabla\right) \bar{U}^{(0)^2} + N_{ij} M_{ij} \bar{U}^{(0)^2} = 0 \tag{39}$$

or

$$\frac{d}{dt}\log[\bar{U}^{(0)^2}] + Tr[NM(t)] = 0. \tag{40}$$

Noting from (28) and (30a) that

$$\frac{\mathrm{d}}{\mathrm{d}t}\log\det A(t) = \mathrm{Tr}(NM),\tag{41}$$

equation (40) can then be solved to get

$$\frac{\bar{U}^{(0)}(t)}{\bar{U}^{(0)}(0)} = \left[\frac{\det A(0)}{\det A(t)}\right]^{1/2}.$$
(42)

In this form, det A(t) can be identified as the Jacobian of the mapping $\bar{x}(0) \rightarrow \bar{x}(t)$. Alternatively, since M(t) is known explicitly from (33), equation (40) can be integrated to yield

$$\bar{U}^{(0)}(t) = \bar{U}^{(0)}(0)/[\det(I + tNM(0))]^{1/2}.$$
(43)

It can also be shown that $\det A(t) \neq 0$ if (1) $\det A(0) \neq 0$, (2) M(0) is symmetric, and (3) Im M(0) is positive definite. These are the same conditions that ensure Im M(t) as positive definite. The method of proof follows that procedure outlined in [5, Appendix B].

3.4. The Gaussian wave packet

The Gaussian wave packet solution follows from (2), (35) and (43) as

$$u(x,t) = U^{(0)}(0)g\left[\frac{\det M(t)}{\det M(0)}\right]^{1/2} \exp\{i\omega[p\cdot(x-\bar{x}) + \frac{1}{2}(x-\bar{x})^{\mathrm{T}}M(t)(x-\bar{x})]\},\tag{44}$$

where $\bar{x} = \bar{x}(t)$ is given in (21), and M(t) in (33).

3.5. Discussion

Given an initial phase slowness vector p and the ray velocity vector c of (16), the center of the GWP propagates according to (21). The shape of the GWP about its center is determined by the tensor M(t), which evolves according to (33). It is shown in (A.15) and (A.19) that N projects onto the plane perpendicular to the phase slowness direction. Therefore, in order to understand the evolution of M, it is useful to define an orthonormal triad $\{d_1, d_2, d_3\}$ such that $d_3 = vp$, and d_1, d_2 are the principal directions of N. With respect to this basis,

$$N = S_1 d_1 d_1^{\mathsf{T}} + S_2 d_2 d_2^{\mathsf{T}}, \tag{45}$$

where S_1 and S_2 have dimensions of (speed)², and shall be called the "spreading factors." Obviously, S_1 and S_2 depend upon the direction of propagation. They may be negative for certain directions in anisotropic media, as illustrated in the example below. By comparison, in an isotropic medium the directions d_1 and d_2 are orthogonal to the ray direction, and $S_1 = S_2 = c^2$, where c is the wave speed.

Define \overline{M}_{ij} , i, j = 1, 2, 3, as the components of M in the basis $\{d_1, d_2, d_3\}$, or

$$\boldsymbol{M} = \bar{\boldsymbol{M}}_{ij} \boldsymbol{d}_i \boldsymbol{d}_j^{\mathsf{T}}. \tag{46}$$

In particular, let M(0) have its principal directions coincide with this basis, so that $\bar{M}(0)$ is diagonal. Then $\bar{M}(t)$ remains diagonal for t > 0, and from (33), (45) and (46)

$$\bar{M}_{11}(t) = \tilde{M}_{11}(0)/[1 + tS_1\bar{M}_{11}(0)], \tag{47a}$$

$$\vec{M}_{22}(t) = \vec{M}_{22}(0)/[1 + tS_2\vec{M}_{22}(0)],$$
 (47b)

$$\bar{M}_{33}(t) = \bar{M}_{33}(0).$$
 (47c)

The form of the GWP remains constant in the phase direction, but it broadens in the orthogonal directions d_1 and d_2 . The widths in these directions depends upon Im $\overline{M}_{11}(t)$ and Im $\overline{M}_{22}(t)$, respectively. The rate of broadening depends upon the values of S_1 and S_2 . Since these generally differ, the GWP will broaden faster in one direction than in the other.

3.6. Numerical example for a transversely isotropic composite

Consider a transversely isotropic composite of parallel cylindrical glass fibers in epoxy matrix, with the fibers 60% of the bulk volume. The composite may be approximated for quasistatic deformation as a homogeneous transversely isotropic solid. The quasistatic approximation should be valid for dynamic wave propagation in the composite if the wave length is much longer than the fiber thickness. This is often the case for ultrasonic studies, and will be assumed here. The constituent parameters are $(\lambda, \mu, \rho) = (13.3, 29.9, 2.55)$ for glass, and (0.89, 1.28, 1.25) for epoxy, where λ and μ are Lamé moduli, ρ density and the units are GPa and gm/cm³, respectively. Assuming the fibers are aligned in the x_1 -direction, this direction is the symmetry axis of the transversely isotropic medium. The effective moduli follow from, for example, the theory of [10] as $(C_{11}, C_{33}, C_{13}, C_{66}, \rho) = (43.4, 10.7, 2.2, 4.4, 2.0)$, in the same units as before.

Figures 1 and 2 show the slowness and wave surfaces of this composite for wave motion polarized in the x_1x_3 -plane, i.e. for qL and qT modes of propagation. These surfaces are defined in Appendix B. Note that the qT surface possesses points of inflection. The qT wave surface has corresponding cusp points. The spreading matrix N is defined explicitly in Appendix B for the three wave types. For wave motion polarized in the plane of x_1x_3 , the eigenvalues S_1 and S_2 of N are $S_2 = N_{22}$ (see (B.17)), and S_1 is the eigenvalue of the 2×2 symmetric matrix of elements N_{11} , N_{13} and N_{33} (see (B.14)-(B.16)). Thus, S_1 is the spreading factor in the x_1x_3 -plane. It is zero at the points of inflection on the qT slowness surface, and becomes negative between these points. Everywhere else it is positive. A plot of S_1 is shown in Fig. 3. The striking feature of this plot is the large variation in the value of S_1 . The corresponding plot for an isotropic solid is two circular arcs, signifying equal spreading in all directions. The present theory is incomplete at the points of inflection on the qT slowness surface. For these discrete directions, the spreading is zero, and the theory predicts no change in the GWP, apart from the spreading associated with S_2 . The pulse then acts like a collimated beam. However, this is not correct for long times. The correct behavior requires a more sophisticated analysis than presently considered. Specifically, we need to look at cubic terms in the phase and higher-order transport terms (see [11] for a relevant discussion).

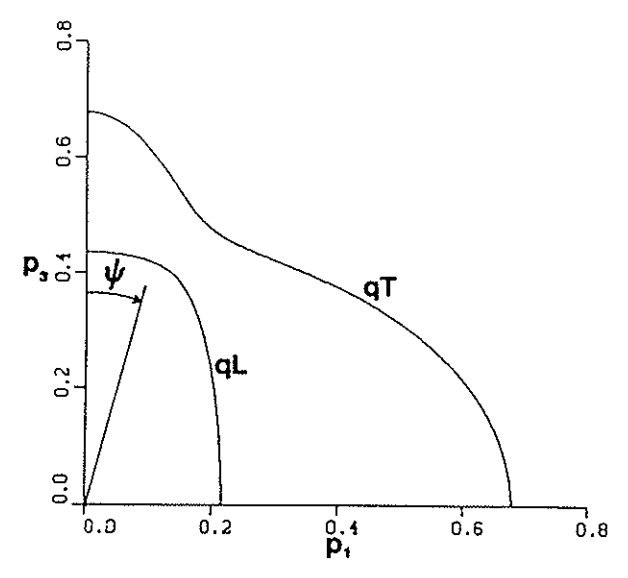


Fig. 1. Slowness surfaces of the qL (inner) and qT (outer) waves in a transversely isotropic solid. The material models a fiber-reinforced, epoxy matrix composite. The fibers are in the x_t-direction, and the units of slowness are μs/mm.

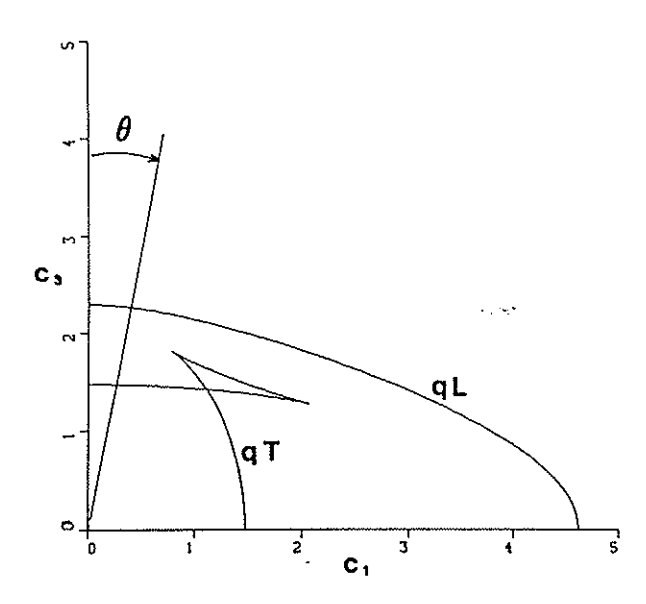


Fig. 2. The wave velocity surfaces corresponding to the slowness surfaces of Fig. 1. Units are mm/µs.

The large variation in spreading is best illustrated by example. Consider a flat ultrasonic transducer bonded to a sample of the composite such that the normal to the transducer face is in the x_1x_3 -plane, and makes an angle ψ with the x_3 -axis. The transducer has a center frequency of 5 MHz, and emits a Gaussian pulse of initial width 5 mm. The initial shape of the pulse is best defined by the matrix \tilde{M} introduced in (60) below. In this configuration, we have

$$\tilde{M}(0) = \text{diag}(\tilde{M}_{11}(0), \tilde{M}_{11}(0), \tilde{M}_{33}(0)).$$

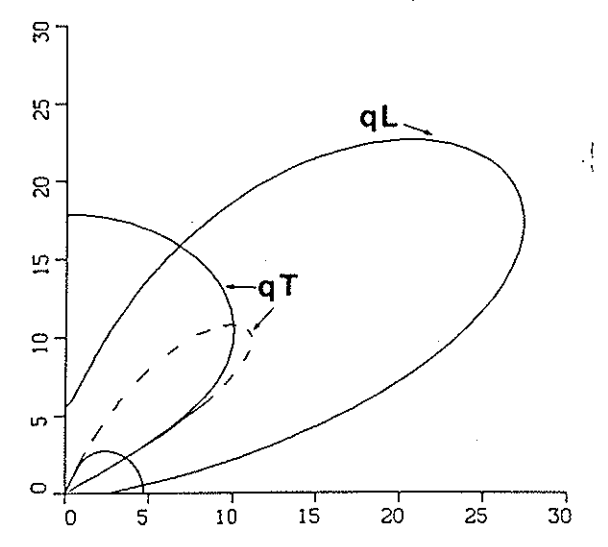


Fig. 3. The spreading factor S_1 which determines the spreading of the pulse in the x_1x_3 -plane of the fiber/epoxy composite. The curves represent the value of S_1 in the direction θ , the ray direction (see Fig. 2). The dashed curve represents where S_1 is negative for the qT wave. Units are mm²/ μ s².

The initial half-width W_0 is defined by $\frac{1}{2}\omega$ Im[$\tilde{M}_{11}(0)$] $W_0^2=1$. With units of length and time in mm and μ s, respectively, this means $\omega=31.4$ and $\tilde{M}_{11}(0)=i/393$. The emitted pulse length is defined by choosing $\tilde{M}_{33}(0)=i/35$. A view of the initial pulse is shown in Fig. 4, $\psi=90^\circ$, t=0. The other plots in Fig. 4 show the radiated qL pulse at t=20 for $\psi=0^\circ$, 20° and 90°. The corresponding ray directions for these values of ψ are $\theta=0^\circ$, 47.4° and 90°, respectively. It is clear from Fig. 4 that the spreading is different in each case, but agrees qualitatively with the qL curve of Fig. 3. Specifically, we note the small spreading when the pulse propagates in the fiber direction ($\psi=90^\circ$). The case $\psi=20^\circ$ is most interesting and corresponds to a large spreading factor S_1 , near the tip of the bulbous curve in Fig. 3. The pulse propagates in a skewed manner, indicating a strong local anisotropy in this direction. Physically, one can understand the skewed shape as the sides of the pulse propagate faster in the fiber direction, causing the rapid broadening in the same direction.

4. Reflection and transmission of GWPs

4.1. Definitions

Let S be a smooth interface separating two homogeneous anisotropic materials. A GWP is defined to be incident on S at time t_0 and at the point x_0 if $x_0 = \bar{x}(t_0)$, where $\bar{x}(t)$ is the ray path of the incident GWP. In other words, t_0 is the time when the center of the pulse hits the interface. Define the interface in the neighborhood of x_0 by the local approximation,

$$x = x_0 + \xi_1 t_1 + \xi_2 t_2 + \sum_{j,l=1,2} \xi_j \xi_l D_{jl} t_3.$$
 (48)

Here, t_1 and t_2 are orthogonal unit tangent vectors to S, and t_3 is a unit normal, such that $\{t_1, t_2, t_3\}$ is a right-hand triad. The parameters ξ_1 and ξ_2 are local uniform coordinates and the 2×2 matrix D defines the local curvature of S.

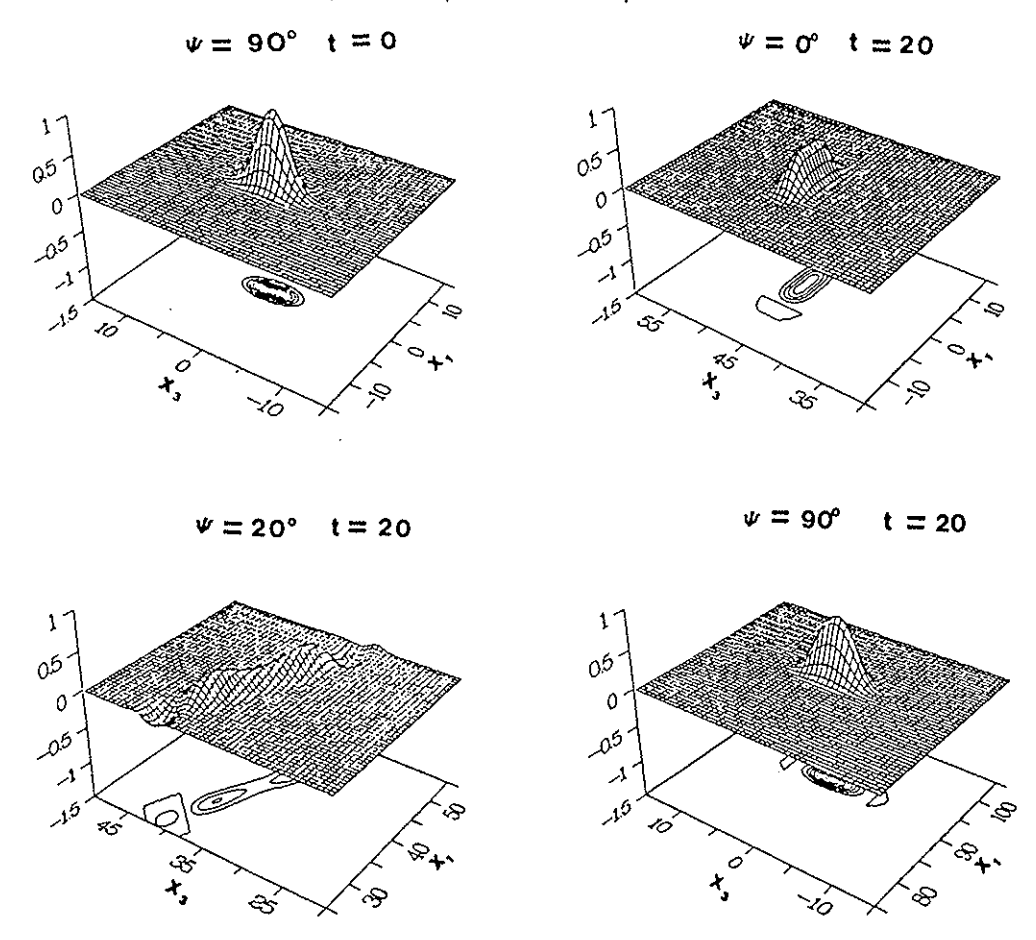


Fig. 4. Plots of a qL pulse propagating in a transversely isotropic medium, approximating a fibre/epoxy composite. The direction of propagation is defined by ψ , the angle the phase velocity makes with the x_3 -axis. The initial pulse is shown for $\psi = 90^\circ$. The initial center is at (0,0). The units are mm and μ s. The plots show the envelope, defined as $u(x,t) \cdot g \exp[-i\omega p \cdot (x - \bar{x}(t))]$. The phase factor $\exp[-i\omega p \cdot (x - \bar{x}(t))]$ removes the oscillations in the p-direction (see (44)) and is included to improve the visual appearance.

Let the incident GWP, denoted by $u^{(1)}$, be of the form given in (44). It is characterized by its slowness vector $p^{(1)}$, with corresponding displacement vector $g^{(1)}$. The amplitude and shape of $u^{(1)}$ at incidence are determined by $U^{(0)I}(t_0)$ and $M^{(1)}(t_0)$. The boundary conditions of continuity of displacement and normal tractions in the neighborhood of (x_0, t_0) are satisfied by introducing reflected and transmitted GWPs. In general, there will be three of each, one corresponding to the quasi-longitudinal (qL) wave and the other two to the quasi-transverse waves (qT1 and qT2) possible on either side of S. Let the reflected and transmitted fields be respectively,

$$\sum_{\alpha = qL, qT1, qT2} u^{(R\alpha)} \tag{49}$$

and

$$\sum_{\alpha=\alpha, l, \alpha T 1, \alpha T^2} u^{(T\alpha)}, \tag{50}$$

where each of these six GWPs has its associated p, g, $U^{(0)}(t_0)$ and $M(t_0)$.

4.2. Determining the slowness vectors

Each of the reflected and transmitted GWPs is of the form of equation (2), or more specifically, equation (44). Define the phase $\phi(x, t)$ of each of these GWPs to equal the incident phase at (x, t_0) . Then, the phases must remain continuous in the neighborhood of (x_0, t_0) on S. This neighborhood is given by (48), therefore there are three first-order conditions:

$$\phi_i$$
, $\partial \phi / \partial \xi_i$, $i = 1, 2$
are continuous at (x_0, t_0) . (51)

These conditions simplify, using (3) and (49), to give that

$$\frac{\partial \phi}{\partial \xi_j} = \nabla \phi \cdot \frac{\partial x}{\partial \xi_j} = p \cdot t_j, \quad j = 1, 2$$
are continuous at (x_0, t_0) . (52)

These two equations determine two components of the slowness vectors. The third component follows from the facts that $\phi_t = -1$ is continuous and that each p satisfies an equation of the form (12). The sign of the third component of p, i.e. $p \cdot t_3$, is obtained by requiring that the associated wave velocity vector c have the appropriate direction. Thus, $c \cdot t_3$ should be of the same sign as $c^{(1)} \cdot t_3$ for the transmitted GWPs, but of opposite sign for the reflected GWPs.

4.3. Determining the displacement vectors and amplitudes

Having found the slowness vector p for each new GWP, the associated wave velocity vector c and unit displacement vector g follow from (6) and (A.8). The continuity of total displacement at (x_0, t_0) then implies

$$U^{(0)I}(t_0)g^{(I)} + \sum_{\alpha = qL, qTI, qT2} U^{(0)R\alpha}(t_0)g^{(R\alpha)} = \sum_{\alpha = qL, qTI, qT2} U^{(0)T\alpha}(t_0)g^{(T\alpha)}.$$
 (53)

Similarly, the continuity of normal traction conditions are

$$C_{ijkl}^{(1)} t_{3j} \left[U^{(0)I}(t_0) g_k^{(I)} p_l^{(I)} + \sum_{\alpha = qL, qT1, qT2} U^{(0)R\alpha}(t_0) g_k^{(R\alpha)} p_l^{(R\alpha)} \right]$$

$$= C_{ijkl}^{(2)} t_{3j} \sum_{\alpha = qL, qT1, qT2} U^{(0)T\alpha}(t_0) g_k^{(T\alpha)} p_l^{(T\alpha)}, \quad i = 1, 2, 3,$$
(54)

where $C^{(1)}$ and $C^{(2)}$ are the elastic moduli tensors on either side of S. The six amplitudes follow from the six equations in (53) and (54).

4.4. The M-tensors of the reflected and transmitted GWPs

The six elements of the complex, symmetric M-tensors follow from the six second-order conditions that ϕ_u , $\partial^2 \phi / \partial t \partial \xi_j$ and $\partial^2 \phi / \partial \xi_i \partial \xi_j$, i, j = 1, 2 are all continuous. The first of these, ϕ_u continuous, implies using (26) that

$$c^{\mathsf{T}}Mc$$
 is continuous. (55)

The second two conditions simplify using (25), (48) and

$$\frac{\partial^2 \phi}{\partial t \, \partial \xi_i} = \nabla \phi_i \cdot \frac{\partial x}{\partial \xi_i} \tag{56}$$

to give

$$c^{\mathsf{T}}Mt_j, \quad j=1,2$$

The final three conditions become, using

$$\frac{\partial^2 \phi}{\partial \xi_i \partial \xi_j} = \left(\frac{\partial x}{\partial \xi_j}\right)^\mathsf{T} \nabla \nabla \phi \left(\frac{\partial x}{\partial \xi_k}\right) + \nabla \phi \cdot \frac{\partial^2 x}{\partial \xi_i \partial \xi_j},\tag{58}$$

(3), (22) and (48), the three conditions

$$\mathbf{t}_{i}^{\mathrm{T}} \mathbf{M} \mathbf{t}_{i} + 2D_{ii} \mathbf{p} \cdot \mathbf{t}_{3}, \quad j, \ k = 1, 2$$

Further simplification of these conditions requires that M be referred to a specific basis. Previously it was shown that the basis $\{d_1, d_2, d_3\}$ is the natural one for considering the evolution of M. In addition, a ray coordinate system may be defined by the orthonormal triad $\{e_1, e_2, e_3\}$, where e_3 is the unit vector in the direction of c. Obviously, these triads coincide for isotropy. There is also the basis $\{t_1, t_2, t_3\}$ defined by the surface S at x_0 . It is not obvious which basis is most advantageous for simplifying the jump conditions. The answer in fact is that none of these is the best, but rather that M be referred to a non-orthogonal basis defined by the triad $\{\bar{e}_1, \bar{e}_2, \bar{e}_3\}$, where $\bar{e}_1 = e_1$, $\bar{e}_2 = e_2$ and $\bar{e}_3 = d_3 = vp$. Thus, define the 3×3 symmetric complex matrix \tilde{M}_{ij} , i, j = 1, 2, 3 by

$$M = \tilde{M}_{ii} \bar{e}_i \bar{e}_i^{\mathsf{T}}. \tag{60}$$

The reason for choosing the non-orthogonal basis $\{\tilde{e}_1, \tilde{e}_2, \tilde{e}_3\}$ will become apparent presently.

The conditions in (55), (57) and (59) indicate that the \tilde{M} -matrix transforms discontinuously from the incident \tilde{M} to the transmitted and reflected matrices. Thus, the individual elements suffer jumps, the values of which are determined by (55), (57) and (59). The first jump condition, (55), implies, using (17), (19) and (60), that

$$v^2 \tilde{M}_{33}$$
 is continuous. (61)

The two jump conditions of (57) imply that

$$v\tilde{M}_{i3}e_i\cdot t_j, \quad j=1,2$$

These conditions simplify, using (51), (52) and (61), to

$$v \sum_{i=1,2} \tilde{M}_{i3} \tilde{e}_i \cdot t_j, \quad j=1,2$$

For each of the bases $\{\bar{e}_1, \bar{e}_2, \bar{e}_3\}$, define the 2×2 transformation matrix Q by

$$Q_{ij} = t_i \cdot \bar{e}_j = t_i \cdot e_j, \quad i, j = 1, 2.$$

$$(64)$$

Thus,

$$\det Q = t_3 \cdot e_3 \tag{65}$$

The jump conditions (63) now become

$$v \sum_{j=1,2} Q_{ij} \tilde{M}_{j3}, \quad i=1,2$$
 are continuous. (66)

The remaining three jump conditions of (59), are, using (64), that

$$\sum_{k,l=1,2} Q_{ik}Q_{jl}\tilde{M}_{kl} + (t_i \cdot \bar{e}_3) \sum_{l=1,2} Q_{jl}\tilde{M}_{l3} + (t_j \cdot \bar{e}_3) \sum_{k=1,2} Q_{ik}\tilde{M}_{k3} + (t_i \cdot \bar{e}_3)(t_j \cdot \bar{e}_3)\tilde{M}_{33} + 2(t_3 \cdot p)D_{ij}, \quad i, j=1, 2$$
are continuous. (67)

These relations simplify further upon noting

$$t_i \cdot \bar{e}_3 = vt_i \cdot p \tag{68}$$

and using the previous conditions of (51), (52), (61) and (66), to give

$$\sum_{k,l=1,2} Q_{ik}Q_{jl}\tilde{M}_{kl} + \frac{2}{v}D_{ij}t_3 \cdot \tilde{e}_3, \quad i, j=1, 2$$
are continuous. (69)

Let α denote any one of the six reflected and transmitted GWPs. Then the six jump conditions can be solved explicitly, from (61), (66) and (69), to give the matrices $\tilde{M}^{(\alpha)} = \tilde{M}^{(\alpha)}(t_0)$ as

$$\tilde{M}_{33}^{(\alpha)} = \frac{v^{(1)2}}{v^{(\alpha)^2}} \tilde{M}_{33}^{(1)},\tag{70a}$$

$$\tilde{M}_{i3}^{(\alpha)} = \frac{v^{(1)}}{v^{(\alpha)}} \sum_{i,k=1,2} Q_{ij}^{(\alpha)^{-1}} Q_{jk}^{(1)} \tilde{M}_{k3}^{(1)}, \quad i = 1, 2,$$
(70b)

$$\tilde{M}_{ij}^{(\alpha)} = \sum_{k,l,m,n=1,2} Q_{ik}^{(\alpha)^{-1}} Q_{jl}^{(\alpha)^{-1}} Q_{km}^{(1)} Q_{ln}^{(1)} \tilde{M}_{mn}^{(1)}
+ 2(t_3 \cdot p^{(1)} - t_3 \cdot p^{(\alpha)}) \sum_{k,l=1,2} Q_{ik}^{(\alpha)^{-1}} Q_{jl}^{(\alpha)^{-1}} D_{kl}, \quad i, j = 1, 2.$$
(70c)

It should now be apparent why we originally chose to represent M in the non-orthogonal basis $\{\bar{e}_1, \bar{e}_2, \bar{e}_3\}$. By so doing, relatively simple equations have been obtained for the new \tilde{M} -matrices. These equations are decoupled as much as possible. Any other choice of basis would result in greater coupling between the coefficient \tilde{M}_{ij} . Note that the form of (70) is very similar to those derived previously for an isotropic medium [7].

4.5. Simplification and localization properties

The six jump conditions of (70) can be written succinctly in matrix form as

$$\tilde{M}^{(\alpha)} = (S^{(\alpha)^{-1}}S^{(1)})\tilde{M}^{(1)}(S^{(\alpha)^{-1}}S^{(1)})^{\mathrm{T}} + 2t_3 \cdot (p^{(1)} - p^{(\alpha)})Q^{(\alpha)^{-1}}DQ^{(\alpha)^{-1}}, \tag{71}$$

where $S^{(\alpha)}$ is the 3×3 matrix associated with the 2×2 matrix $Q^{(\alpha)}$,

$$S^{(\alpha)} \equiv \begin{bmatrix} Q^{(\alpha)} & 0\\ 0 & v^{(\alpha)} \end{bmatrix}. \tag{72}$$

Also, the last term in (71), which represents a 2×2 matrix must be understood to apply only to the i, j = 1, 2 elements of $\tilde{M}^{(\alpha)}$. This term is identically zero if the interface is locally flat at the point of incidence. Note that it is preferable to express M in the basis $\{d_1, d_2, d_3\}$ for the purposes of calculating the evolution of the M-tensors before and after incidence. The required transformations $\bar{M} \leftrightarrow \hat{M}$ is

$$\bar{M} = V\tilde{M}V^{\mathsf{T}},\tag{73}$$

where the 3×3 matrix V is

$$V_{ij} = d_i \cdot \bar{e}_j. \tag{74}$$

Using the facts that $c = ce_3$ and $p = v^{-1}d_3$, it is easy to deduce from (17) and (74) that det V = v/c, and

$$V^{-1} = \frac{c}{v} \begin{bmatrix} d_2 \cdot e_2 & -d_1 \cdot e_2 & 0 \\ -d_2 \cdot e_1 & d_1 \cdot e_1 & 0 \\ d_1 \cdot e_3 & d_2 \cdot e_3 & v/c \end{bmatrix}.$$
 (75)

Now combine (71) and (74) to obtain an expression for the six jump conditions $\tilde{M}^{(1)} \to \tilde{M}^{(\alpha)}$. In particular, for a locally flat interface (D=0),

$$\bar{M}^{(\alpha)} = [V^{(\alpha)}S^{(\alpha)^{-1}}S^{(1)}V^{(1)^{-1}}]\bar{M}^{(1)}[V^{(\alpha)}S^{(\alpha)^{-1}}S^{(1)}V^{(1)^{-1}}]^{\mathrm{T}}.$$
(76)

Several useful results are apparent from this relation. First, it is clear that $M^{(\alpha)}$ will be symmetric if $M^{(1)}$ is symmetric. Secondly, since (76) represents a linear transformation, and the matrices in square brackets in (76) are all real, it is clear that the real matrices $\operatorname{Im} \bar{M}^{(\alpha)}$ satisfy similar transformations. In fact, the imaginary part of (76) represents the correct transformation $\operatorname{Im} \bar{M}^{(1)} \to \operatorname{Im} \bar{M}^{(\alpha)}$ even for curved interfaces, since the extra terms necessary in this equation are real. Thus, $\operatorname{Im} \bar{M}^{(\alpha)}$ is positive definite if $\operatorname{Im} \bar{M}^{(1)}$ is positive definite. But the latter is a necessary condition, expressing the fact that the incident GWP is localized. Hence, the reflected and transmitted GWPs are also localized.

Finally, define the angle $\theta^{(\alpha)}$ that the ray direction of the GWP of type α makes with the interface normal,

$$\cos\,\theta^{(\alpha)} = t_3 \cdot e_3^{(\alpha)}. \tag{77}$$

Equation (77), along with (64), (72) and det $V^{(\alpha)} = v^{(\alpha)}/c^{(\alpha)}$, implies that for incidence upon an arbitrarily curved interface,

$$\frac{\det \operatorname{Im} M^{(\alpha)}}{\det \operatorname{Im} M^{(1)}} = \left[\frac{c^{(1)} \cos \theta^{(1)}}{c^{(\alpha)} \cos \theta^{(\alpha)}} \right]^{2}. \tag{78}$$

The ratio of complex numbers, $\det M^{(\alpha)}/\det M^{(1)}$ is equal to the real ratio in (78) if the interface is locally flat.

4.6. Two-dimensional simplification

The general results simplify considerably if the transmission/reflection process possesses a plane of symmetry. This occurs if the incident pulse, material anisotropies and interface are such that $d_2^{(\alpha)} = e_2^{(\alpha)} = t_2$ for each α . The local interface geometry is depicted in Fig. 5, which shows the ray and phase vectors for the incident and a single transmitted GWP. The local radii of curvature of the interface are a_1 in the plane of Fig. 5, and a_2 in the plane of t_2 and t_3 . The matrix D of (48) is $D = \text{diag}(1/2a_1, 1/2a_2)$. It will be assumed, for further simplicity, that $\bar{M}_{12}^{(1)} = \bar{M}_{23}^{(1)} = 0$, and hence, $\tilde{M}_{12}^{(1)} = \tilde{M}_{23}^{(1)} = 0$. The results presented here will be used in the example of Section 4.8.

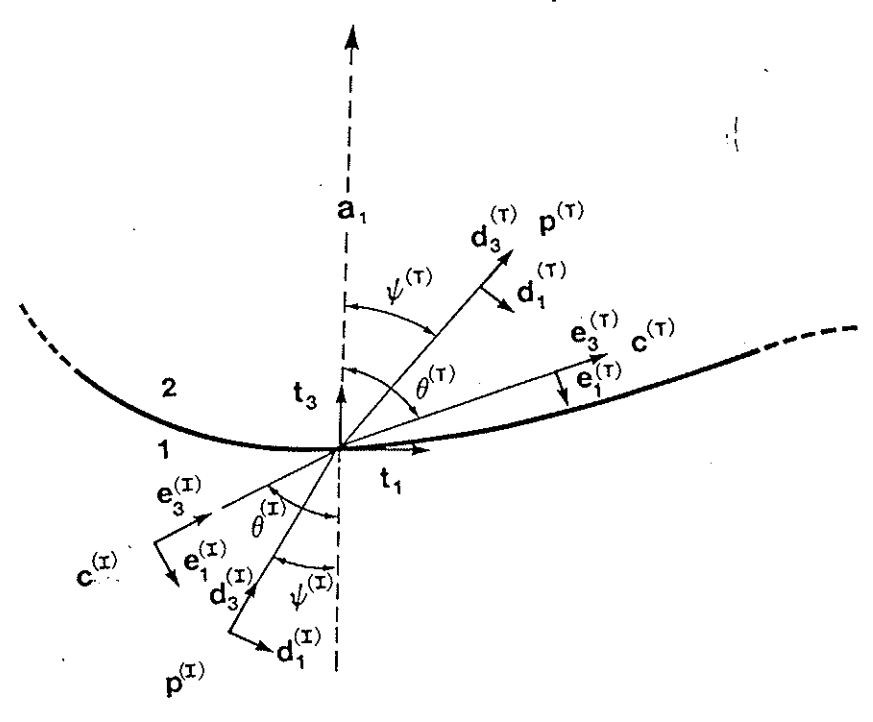


Fig. 5. A two-dimensional illustration of the reflection/transmission of a Gaussian wave packet from an interface. The incident pulse and one of the transmitted pulses are considered.

The relations in (70) reduce to $\tilde{M}_{12}^{(\mathrm{T})} = \tilde{M}_{23}^{(\mathrm{T})} = 0$, and

$$\tilde{M}_{33}^{(T)} = \frac{v^{(1)^2}}{v^{(T)^2}} \tilde{M}_{33}^{(1)}, \tag{79a}$$

$$\tilde{M}_{13}^{(T)} = \frac{v^{(1)}\cos\theta^{(1)}}{v^{(T)}\cos\theta^{(T)}}\,\tilde{M}_{13}^{(I)},\tag{79b}$$

$$\tilde{M}_{11}^{(T)} = \frac{\cos^2 \theta^{(1)}}{\cos^2 \theta^{(T)}} \tilde{M}_{11}^{(1)} + \frac{1}{a_1 \cos^2 \theta^{(T)}} \left(\frac{\cos \psi^{(1)}}{v^{(1)}} - \frac{\cos \psi^{(T)}}{v^{(T)}} \right), \tag{79c}$$

$$\tilde{M}_{22}^{(T)} = \tilde{M}_{22}^{(1)} + \frac{1}{a_2 \cos^2 \theta^{(T)}} \left(\frac{\cos \psi^{(1)}}{v^{(1)}} - \frac{\cos \psi^{(T)}}{v^{(T)}} \right). \tag{79d}$$

Following the notation of Musgrave [1], let Δ be the angle between the ray and phase directions:

$$\Delta = \theta - \psi. \tag{80}$$

The matrix V of (74) is now \cdot

$$V = \begin{bmatrix} \cos \Delta & 0 & 0 \\ 0 & 1 & 0 \\ -\sin \Delta & 0 & 1 \end{bmatrix},\tag{81}$$

The relation between the matrices $\bar{M}^{(1)}$ and $\bar{M}^{(T)}$ defined in the phase vector system (d_1, d_2, d_3) , follows from eqs. (74), (79) and (81). Define

$$\alpha = \frac{\cos \Delta^{(T)} \cos \theta^{(I)}}{\cos \Delta^{(I)} \cos \theta^{(T)}}, \qquad \beta = \frac{v^{(I)}}{v^{(T)}}, \tag{82a, b}$$

$$\gamma = \frac{\cos \theta^{(1)}}{\cos \Delta^{(1)} \sin \psi^{(T)}} \left[\frac{\sin \Delta^{(1)} \sin \gamma^{(1)}}{\cos \theta^{(1)}} - \frac{\sin \Delta^{(T)} \sin \psi^{(T)}}{\cos \theta^{(T)}} \right], \tag{82c}$$

$$\delta = \sec^2 \theta^{(T)} \left(\frac{\cos \psi^{(1)}}{v^{(1)}} - \frac{\cos \psi^{(T)}}{v^{(T)}} \right), \tag{82d}$$

then

$$\bar{M}_{11}^{(T)} = \alpha^2 \bar{M}_{11}^{(1)} + \frac{\delta}{a_1} \cos^2 \Delta^{(T)}, \tag{83a}$$

$$\bar{M}_{13}^{(T)} = \alpha \beta \bar{M}_{13}^{(1)} + \alpha \gamma \bar{M}_{11}^{(1)} - \frac{\delta}{a_1} \sin \Delta^{(T)} \cos \Delta^{(T)}, \tag{83b}$$

$$\bar{M}_{33}^{(T)} = \beta^2 \bar{M}_{33}^{(1)} + 2\beta \gamma \bar{M}_{13}^{(1)} + \gamma^2 \bar{M}_{11}^{(1)} + \frac{\delta}{a_1} \sin^2 \Delta^{(T)}, \tag{83c}$$

$$\bar{M}_{22}^{(T)} = \bar{M}_{22}^{(1)} + \frac{\delta}{a_2} \cos^2 \theta^{(T)}.$$
 (83d)

Note that Δ is zero in an isotropic medium. Hence, $\gamma = 0$ of both materials are isotropic, in which case the coupling between \bar{M} -elements disappears [5, 7].

4.7. Discussion

The general results in (79) and (83) for the two-dimensional configuration are for an arbitrary incident Gaussian wave packet. The latter result, (83), is defined in the phase slowness vector system $\{d_1, d_2, d_3\}$ which, as discussed in Subsection 3.4 above, is the natural basis for considering the evolution of the M-tensors on either side of the interface. However, the jump conditions are best understood by considering (79) for M referred to the non-orthogonal basis $\{e_1, e_2, d_3\}$.

To see this, consider two extreme limits for the incident pulse. The first is that of a very short pulse for which Im $\tilde{M}_{33}^{(1)} \gg \text{Im } \tilde{M}_{11}^{(1)}$, Im $\tilde{M}_{13}^{(1)}$. This is equivalent to a delta-function wavefront, oriented perpendicular to the phase slowness direction $d_3^{(1)}$. The transmitted pulse, from (79), also satisfies Im $\tilde{M}_{33}^{(T)} \gg \text{Im } \tilde{M}_{11}^{(T)}$, Im $\tilde{M}_{13}^{(T)}$. Hence, it is also a propagating singularity oriented perpendicular to its phase direction. This limit is analogous to considering wavefronts of infinitely wide plane waves [1].

The other extreme is an incident pulse that is very long in the wave velocity direction $e_3^{(1)}$, i.e., Im $\tilde{M}_{11}^{(1)} \gg \text{Im } \tilde{M}_{33}^{(1)}$, Im $\tilde{M}_{13}^{(1)}$, and thus the transmitted pulse is a long, pencil-shaped object oriented in the new wave direction $e_3^{(T)}$.

For these two limiting cases, the principal directions of both the incident and scattered pulses are defined by the basis $\{d_1, d_2, d_3\}$ of the slowness vector in the first instance, and by the basis $\{e_1, e_2, e_3\}$ of the wave velocity vector in the second. This relative simplicitly disappears for an incident pulse that is neither very short nor very long. For example, if the incident pulse is oriented in the directions d_1, d_2 and d_3 ($\bar{M}_{13}^{(1)} = 0$ in (83)) and the interface is flat $(a_1^{-1} = a_2^{-1} = 0)$, then (83) shows that the transmitted \bar{M}

is

$$\bar{\boldsymbol{M}}^{(\mathsf{T})} = \begin{bmatrix} \alpha^2 \bar{M}_{11}^{(\mathsf{I})} & 0 & \alpha \gamma \bar{M}_{11}^{(\mathsf{I})} \\ 0 & \bar{M}_{22}^{(\mathsf{I})} & 0 \\ \alpha \gamma \bar{M}_{11}^{(\mathsf{I})} & 0 & \beta^2 \bar{M}_{33}^{(\mathsf{I})} + \gamma^2 \bar{M}_{11}^{(\mathsf{I})} \end{bmatrix}. \tag{84}$$

The principal directions of the envelope of the transmitted pulse are defined by the eigenvectors of $Im M^{(T)}$, which from (84), are obviously dependent upon α and γ . Note that for isotropic media [5, 7], $\gamma \equiv 0$, and so the matrix $\tilde{M}^{(T)} \equiv \tilde{M}^{(T)}$ is diagonal.

4.8. Example: Transmission from a fluid into a transversely isotropic solid

As an illustration of transmission consider a wave packet originating in water, incident upon the transversely isotropic glass/epoxy composite material discussed in Section 3.6. Using the same coordinate axes as there, let the solid occupy $x_3 > 0$, the fluid $x_3 < 0$, with the flat interface on $x_3 = 0$. The initial packet is the same, with the initial packet center at a distance of 15 mm from the origin. Since the sound speed is 1.5 mm/ μ s, the packet center is incident upon the interface at $t = 10\mu$ s, and the point of incidence is the origin. The initial direction of propagation is in the x_1x_3 -plane, and makes an angle θ with the interface normal, see Fig. 5.

The results of Section 4.6 apply here. Two transmitted packets are generated, a qL and a qT, each with its propagation direction in the x_1x_3 -plane. These directions can be estimated for a given θ from Fig. 1. To do this use $p_1 = \frac{2}{3} \sin \theta$, the ray directions then correspond to the directions of the normals to the slowness surfaces. Figures 6-8 show the transmitted packets at $t = 20 \,\mu s$, for $\theta = 5^{\circ}$, 10° and 15°. The qL and qT packets are shown separately for clarity. It is clear from the positions of the packet centers in these figures that the wave speeds vary with propagation direction, as expected. Note the orientation of the packets, in agreement with the discussion above for a short pulse. Probably the most interesting feature in these figures is the large variation in the spreading. This may be understood on the basis of the spreading factor of Fig. 3. For the material considered, the spreading factor is a very sensitive function of the propagation direction, and this sensitivity is reflected in the results of Figs. 6-8.

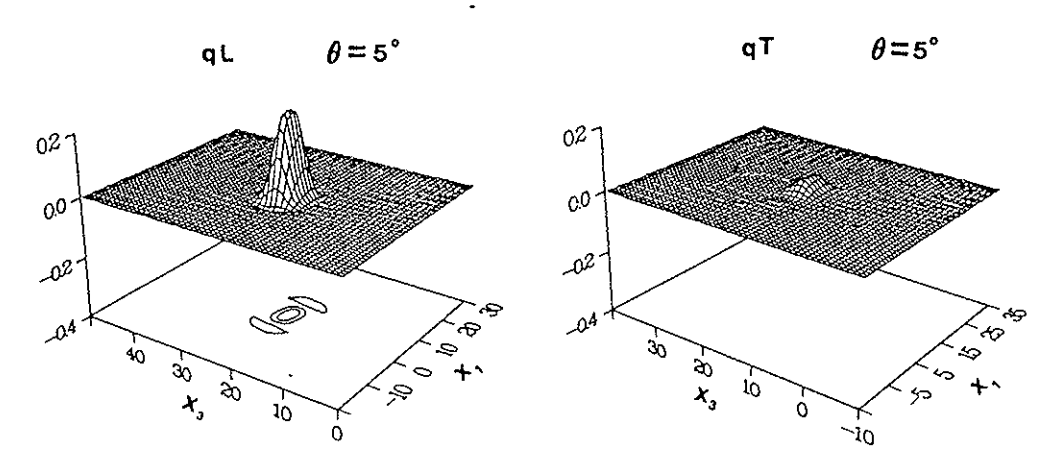


Fig. 6. The qL and qT transmitted pulses for $\theta = 5^{\circ}$, 10 μ s after incidence at $x_1 = x_3 = 0$ into the transversely isotropic material. The plotted surfaces show the envelopes, defined as $u(x, t) \cdot g \exp[-i\omega p \cdot (x - \bar{x}(t))]$ for the separate wave packets.

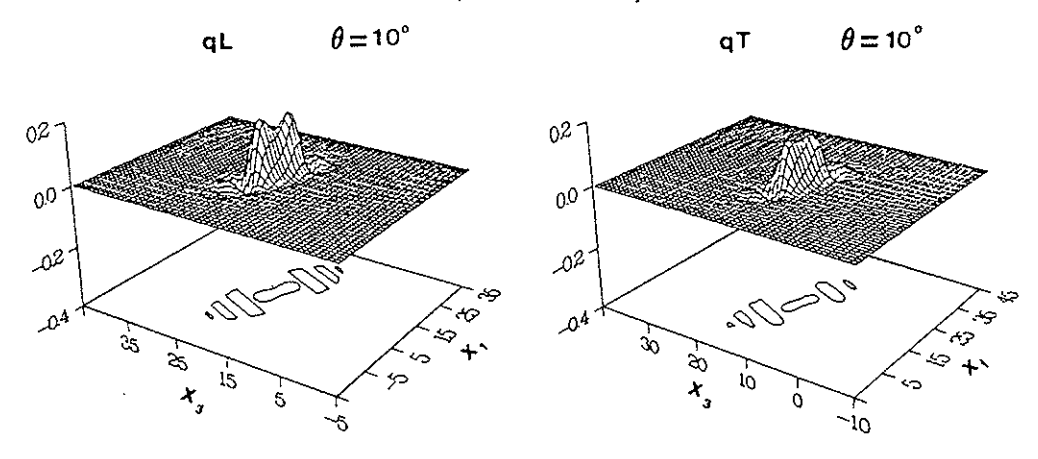


Fig. 7. The same as Fig. 6, but for $\theta = 10^{\circ}$. Note the increased lateral spreading in comparison with Fig. 6.

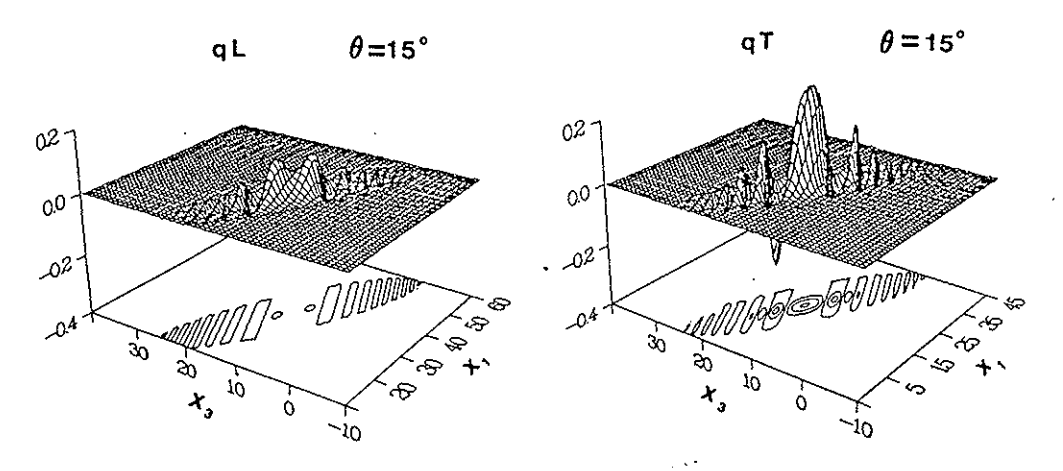


Fig. 8. The same as Figs. 6 and 7, but for $\theta = 15^{\circ}$.

5. Conclusions

A general theory has been given for the propagation and scattering of compact, Gaussian shaped pulses in piecewise homogeneous anisotropic solids. The general solution is described by (44), where the evolution of the envelope tensor M is given in (33). The form of this pulse solution is relatively simple, considering that it is explicitly time-dependent and localized. This simplicity makes the theory ideal for modeling the propagation of ultrasonic pulses. The evolution of the propagating pulse is characterized by a spreading matrix N. The eigenvalues of N define the rate of broadening, and these rates can vary significantly with direction, as shown by example. Therefore, it is necessary to characterize N for a given material in order to understand the propagation of pulses through it. Explicit equations have been given for the elements of this matrix. The reflection/transmission problem of a pulse incident upon a smooth interface has also been discussed and the necessary jump conditions for M derived. The properties of the transmitted and reflected pulses are fundamentally different than for isotropic media.

Acknowledgment

Thanks to B. White for useful discussions. This work was supported by the National Science Foundation, through Grant No. MDM 85-16256.

Appendix A. The wave velocity vector and related quantities

Define the tensor

$$\Gamma_{ij} = \rho^{-1} C_{kijl} p_k p_l. \tag{A.1}$$

The secular equation (7) can then be written, using (8), as

$$D_{kl}(\Gamma_{kl} - f^2 \delta_{kl}) = 0, \tag{A.2}$$

where

$$D_{ij} = \frac{1}{6} e_{ikl} e_{jmn} (\Gamma_{km} - f^2 \delta_{km}) (\Gamma_{ln} - f^2 \delta_{ln})$$
(A.3)

and e_{ijk} is the third-order alternating tensor, $e_{123} = 1$, $e_{132} = -1$, $e_{122} = 0$, etc. Differentiating (A.2) gives,

$$2f\frac{\partial f}{\partial p_i} = \frac{D_{mn}}{D_{kk}} \frac{\partial \Gamma_{mn}}{\partial p_i}.$$
(A.4)

The wave velocity vector c then follows from (15), (16) and (A.4) as

$$c_i = \rho^{-1} C_{ijkl} p_l \bar{D}_{jk} / \bar{D}_{mm}, \tag{A.5}$$

where $\bar{D}_{ij} \equiv D_{ij} \ (f=1)$.

It then follows from (15), (A.1), (A.2) and (A.5) that

$$p_i c_i = \Gamma_{ij} \bar{D}_{ij} / \bar{D}_{nm} = 1. \tag{A.6}$$

A more transparent expression exists for c. Let g be the unit eigenvector of (6). It then follows from (A.2) that

$$g_i g_j = \bar{D}_{ij} / \bar{D}_{kk}. \tag{A.7}$$

The wave speed may now be written from (A.5) as

$$c_i = \rho^{-1} C_{ijkl} g_j g_k p_l \tag{A.8}$$

An expression for N of (31) follows by rewriting (A.4) using (A.7) as

$$\frac{\partial f}{\partial p_i} = \frac{1}{2f} g_k g_l \frac{\partial \Gamma_{kl}}{\partial p_i}.$$
(A.9)

Then,

$$\frac{\partial^2 f}{\partial p_i \, \partial p_j} = \frac{1}{2f} g_k g_l \frac{\partial^2 \Gamma_{kl}}{\partial p_i \, \partial p_j} - \frac{1}{f} \frac{\partial f}{\partial p_i} \frac{\partial f}{\partial p_j} + \frac{1}{2f} \frac{\partial \Gamma_{kl}}{\partial p_i} \frac{\partial g_k g_l}{\partial p_j}. \tag{A.10}$$

Putting f = 1 in (A.10), and using (16) and (A.1),

$$N_{ij} = \rho^{-1} C_{iklj} g_k g_l - c_i c_j + C_{mklj} p_k \frac{\partial}{\partial p_i} (g_m g_l). \tag{A.11}$$

Let us rewrite this as

$$N = N^{(1)} + N^{(2)}, (A.12)$$

where

$$N_{ij}^{(1)} = \rho^{-1} C_{ikjl} g_k g_l - c_i c_j, \tag{A.13}$$

$$N_{ij}^{(2)} = \frac{1}{2} \frac{\partial \Gamma_{kl}}{\partial p_i} \frac{\partial g_k g_l}{\partial p_i}. \tag{A.14}$$

It is clear that $N^{(1)}$ is symmetric. Also, from (A.6), (A.8) and (A.13),

$$N_{ij}^{(1)} p_j = 0. (A.15)$$

The symmetry of $N^{(2)}$ is not immmediately apparent, but will be demonstrated shortly. Noting

$$p_i \frac{\partial \Gamma_{kl}}{\partial p_i} = 2\Gamma_{kl},\tag{A.16}$$

it follows that

$$N_{ij}^{(2)} p_i = \Gamma_{kl} \frac{\partial g_k g_l}{\partial p_j}. \tag{A.17}$$

Differentiating (A.2), using (A.7), gives

$$(\Gamma_{kl} - f^2 \delta_{kl}) \frac{\partial g_k g_l}{\partial p_j} + \left(g_k g_l \frac{\partial \Gamma_{kl}}{\partial p_j} - 2c_j \right) = 0. \tag{A.18}$$

Equations (A.18), (A.17), (A.1) and (A.8), along with $g_k g_k = 1$, imply

$$N_{ij}^{(2)} p_i = 0. (A.19)$$

Thus, both $N^{(1)}$ and $N^{(2)}$, and hence N, are projection tensors onto the plane perpendicular to the phase slowness vector p.

The equation for $N^{(1)}$ in (A.13) can be made explicit through the use of (A.7) and (A.8), once the slowness surface is determined from (A.2). The matrix $N^{(2)}$ still needs to be simplified. From its definition in (A.14), and (A.7), (A.8),

$$N_{ij}^{(2)} = \frac{1}{2D_{qq}} \left[\frac{\partial D_{mn}}{\partial p_j} \frac{\partial \Gamma_{mn}}{\partial p_i} - 2c_i \frac{\partial D_{mm}}{\partial p_j} \right]_{f=1}.$$
 (A.20)

From (A.3) and the definition $\bar{D}_{ij} = D_{ij}$ (f=1),

$$\left. \frac{\partial D_{mn}}{\partial p_j} \right|_{f=1} = \frac{\partial \overline{D}_{mn}}{\partial p_j} - \frac{2}{3} \left[(\Gamma_{qq} - 2) P_{mn} - \Gamma_{mn} \right] c_j, \tag{A.21}$$

$$\frac{\partial D_{mn}}{\partial p_j} \frac{\partial \Gamma_{mn}}{\partial p_i} \bigg|_{f=1} = \frac{\partial \bar{D}_{mn}}{\partial p_j} \frac{\partial \Gamma_{mn}}{\partial p_i} - 2c_j \frac{\partial \bar{D}_{mm}}{\partial p_i}. \tag{A.22}$$

Equations (A.20)-(A.22) give an explicit formula for $N^{(2)}$:

$$N_{ij}^{(2)} = \left[\frac{1}{2} \frac{\partial \vec{D}_{mn}}{\partial p_j} \frac{\partial \Gamma_{mn}}{\partial p_i} - \left(c_i \frac{\partial \vec{D}_{mm}}{\partial p_j} + c_j \frac{\partial \vec{D}_{mm}}{\partial p_i} \right) + \frac{4}{3} c_i c_j (\Gamma_{mm} - 3) \right] / \vec{D}_{qq}. \tag{A.23}$$

The symmetry of $N^{(2)}$ is apparent from (A.23).

A matrix related to N occurs in the paper by Cerveny [9]. An examination of that paper shows that the matrix $F_{ij}^{(2)}/2D$ in [9, eq. (34)] should be identical to N_{ij} . However, using his [9, eq. (35)], it can be shown that

$$F_{ij}^{(2)}/2D = N_{ij} + c_i c_j + \left[c_j \frac{\partial \bar{D}_{mm}}{\partial p_i} - \frac{4}{3}c_i c_j (\Gamma_{mm} - 3)\right] / \bar{D}_{qq},$$
 (A.24)

where the right-hand side of this equation uses the present notation. The discrepancy between the two results is due to Cerveny's failure to properly include the implicit derivatives, as in (A.21) and (A.22).

Appendix B. Transverse isotropy

Let the x_1 -axis be the zonal axis or axis of symmetry. The five independent elastic moduli are C_{11} , C_{33} , C_{13} , C_{23} and C_{66} . See Musgrave [1] and Payton [4] for a complete discussion of the slowness and wave surfaces. Without loss of generality, we take $p_2 = 0$.

The purely transverse TH wave is polarized in the x_2 -direction, i.e., g = (0, 1, 0). Then

$$f(p) = (A^2 p_1^2 + B^2 p_3^2)^{1/2}, \tag{B.1}$$

where

$$A = (C_{66}/\rho)^{1/2},\tag{B.2}$$

$$B = (C_{44}/\rho)^{1/2},\tag{B.3}$$

$$C_{44} = \frac{1}{2}(C_{33} - C_{23}),\tag{B.4}$$

and f(p) = 1 defines the slowness surface, in this case a spheroid. Explicit differentiation of (B.1) gives the wave velocity form (16) as

$$c = (A^2 p_1, 0, B^2 p_3)$$
 (B.5)

and the spreading matrix, from (31), as

$$N = A^{2}B^{2} \begin{bmatrix} p_{3}^{2} & 0 & -p_{1}p_{3} \\ 0 & A^{-2} & 0 \\ -p_{1}p_{3} & 0 & p_{1}^{2} \end{bmatrix}.$$
 (B.6)

The quasi-longitudinal (qL) and quasi-transverse (qT) waves have their displacement eigenvectors in the x_1x_3 -plane and are defined by $f_+=1$ and $f_-=1$, respectively, where

$$f_{\pm}(p) = \left[1 + \frac{D}{2} \pm \frac{D^{1/2}}{2} \left(D + 2 - 2Ep_1^2 - 2Fp_3^2 - 4Gp_1p_3\right)^{1/2}\right]^{1/2}$$
(B.7)

and

$$D = [(C_{11} + C_{66})p_1^2 + (C_{33} + C_{66})p_3^2]/\rho - 2,$$
(B.8)

$$E = \{ [2C_{11}C_{66}p_1^2 + (C_{11}C_{33} + C_{66}^2)p_3^2]/\rho^2 - (C_{11} + C_{66})/\rho \}/D,$$
(B.9)

$$F = \{ [2C_{22}C_{66}p_3^2 + (C_{11}C_{33} + C_{66}^2)p_1^2]/\rho^2 - (C_{33} + C_{66})/\rho \}/D,$$
(B.10)

$$G = (C_{13} + C_{66})^2 p_1 p_3 / \rho^2 D.$$
(B.11)

The wave velocity vector is $c = (c_1, 0, c_3)$, where

$$c_1 = p_1 E + p_3 G,$$
 (B.12)

$$c_3 = p_1 G + p_3 F.$$
 (B.13)

The elements of the matrix N follow from Appendix A:

$$N_{11} = E - c_1^2 + \{ [4C_{11}C_{66}p_1^2 - (C_{13} + C_{66})^2p_3^2]/\rho^2 - 4c_1p_1(C_{11} + C_{66})/\rho + 4c_1^2 \}/D,$$
 (B.14)

$$N_{33} = F - c_3^2 + \{ [4C_{33}C_{66}p_3^2 - (C_{13} + C_{66})^2p_1^2] / \rho^2 - 4c_3p_3(C_{33} + C_{66}) / \rho + 4c_3^2 \} / D,$$
 (B.15)

$$N_{13} = 2G - c_1c_3 + 2\{p_1p_3(C_{11}C_{13} + C_{66}^2)/\rho^2$$

$$-[c_1p_3(C_{33}+C_{66})+c_3p_1(C_{11}+C_{66})]/\rho+2c_1c_3\}/D,$$
(B.16)

$$N_{22} = c_3/p_3, (B.17)$$

$$N_{12} = N_{21} = 0. ag{B.18}$$

Several simplifying cases should be noted for (B.14)-(B.18). First, let $p_3 = 0$ for the qL wave. Then $c_3 = 0$, $c_1 = 1/p_1 = (C_{11}/\rho)^{1/2}$ and $N = \text{diag}(0, N_{22}, N_{22})$, where

$$N_{22} = [C_{66} + (C_{13} + C_{66})^2 / (C_{11} - C_{66})] / \rho.$$
(B.19)

This represents the spreading of the pure L-wave propagating in the direction of the zonal axis. Second, let $p_3 = 0$ for the qT wave. Then this is a pure transverse wave with $c_3 = 0$, $c_1 = 1/p_1 = (C_{66}/\rho)^{1/2}$ and $N = \text{diag}(0, N_{22}, N_{22})$, where

$$N_{22} = \left[C_{23} - (C_{13} + C_{66})^2 / (C_{11} - C_{66}) \right] / \rho \tag{B.20}$$

Note that for both the qL and qT waves in the x_1 -direction, the matrix N has degenerate eigenvectors in the x_2x_3 -plane. This is to be expected from the symmetry. However, the N matrix for the qT wave is not the same as N for the TH mode of (B.6), which is $N = \text{diag}(0, B^2, B^2)$. Thus, while the transverse wave slowness surfaces coalesce at $p_2 = p_3 = 0$, the local curvatures of the surfaces are different.

The qL and qT modes also become pure modes if $p_1 = 0$. For the qL mode, we then have $c_1 = 0$, $c_3 = 1/p_3 = (C_{33}/\rho)^{1/2}$ and $N = \text{diag}(N_{11}, N_{22}, 0)$ with

$$N_{11} = [C_{66} + (C_{13} + C_{66})^2 / (C_{33} - C_{66})] / \rho,$$
(B.21)

$$N_{22} = C_{33}/\rho.$$
 (B.22)

For the qT mode, $c_1 = 0$, $c_3 = 1/p_3 = (C_{66}/\rho)^{1/2}$, $N = \text{diag}(N_{11}, N_{22}, 0)$ and

$$N_{11} = \left[C_{11} - (C_{13} + C_{66})^2 / (C_{33} - C_{66}) \right] / \rho, \tag{B.23}$$

$$N_{22} = C_{66}/\rho.$$
 (B.24)

Appendix C. Transverse isotropy transmission coefficients

Reflection and transmission coefficients for a wave incident from an inviscid fluid upon a transversely isotropic solid are presented. The situation is as depicted in Fig. 5, with medium 1 the fluid, and medium 2 the transverse solid with the axis of symmetry in the x_1 -direction. One reflected wave is generated in the fluid. A quasi-transverse (qT) and quasi-longitudinal (qL) pair of waves are transmitted into the solid.

Referring to Section 4.3, the incident and reflected waves are defined by

$$\mathbf{g}^{(1)} = (\sin \theta^{(1)}, 0, \cos \theta^{(1)}), \tag{C.1}$$

$$p^{(1)} = c_1^{-1}(\sin \theta^{(1)}, 0, \cos \theta^{(1)}), \tag{C.2}$$

$$g^{(R)} = (\sin \theta^{(I)}, 0, -\cos \theta^{(I)}),$$
 (C.3)

$$\mathbf{p}^{(R)} = c_{\epsilon}^{-1} (\sin \theta^{(1)}, 0, -\cos \theta^{(1)}), \tag{C.4}$$

where c_f is the fluid sound speed. The transmitted slownesses are

$$p^{(T\alpha)} = (p_1^{(T\alpha)}, 0, p_3^{(T\alpha)}), \quad \alpha = qL, qT,$$
 (C.5)

where Snell's law dictates that

$$p_1^{(TqL)} = p_1^{(TqT)} = p_1^{(1)} \equiv p_1.$$
 (C.6)

The slowness components $p_3^{(T\alpha)}$, $\alpha = qL$, qT, then follow from Appendix B. The transmitted unit displacement vectors are

$$g^{(T\alpha)} = (G_1^{(T\alpha)}, 0, G_3^{(T\alpha)}) / [G_1^{(T\alpha)^2} + G_3^{(T\alpha)^2}]^{1/2}, \quad \alpha = qL, qT,$$
(C.7)

where

$$G_1^{(T\alpha)} = \rho^{-1} (C_{13} + C_{66}) p_1 p_3^{(T\alpha)}, \quad \alpha = qL, qT,$$
 (C.8)

$$G_3^{(\mathsf{T}\alpha)} = 1 - \rho^{-1} C_{11} p_1^2 - \rho^{-1} C_{66} p_3^{(\mathsf{T}\alpha)^2}, \quad \alpha = \mathsf{qL}, \mathsf{qT}. \tag{C.9}$$

The reflected and transmitted amplitudes are then (see Section 4.3),

$$\begin{bmatrix} U^{(0)R} \\ U^{(0)TqL} \\ U^{(0)TqT} \end{bmatrix} = U^{(0)I} \begin{bmatrix} \cos \theta^{(I)} & g_3^{(TqL)} & g_3^{(TqT)} \\ -\rho_I c_I & P^{(qL)} & P^{(qT)} \\ 0 & Q^{(qL)} & Q^{(qT)} \end{bmatrix}^{-1} \begin{bmatrix} \cos \theta^{(I)} \\ \rho_I c_I \\ 0 \end{bmatrix},$$
(C.10)

where

$$P^{(\alpha)} = C_{13} p_1 g_1^{(T\alpha)} + C_{33} p_3^{(T\alpha)} g_3^{(T\alpha)}, \quad \alpha = qL, qT,$$
(C.11)

$$Q^{(\alpha)} = p_3^{(T\alpha)} g_1^{(T\alpha)} + p_1 g_3^{(T\alpha)}, \quad \alpha = qL, qT,$$
(C.12)

and ρ_{ℓ} is the fluid density. Equation (C.10) follows from the continuity of σ_{13} , σ_{33} and u_3 at the interface.

References

- [1] M.J.P. Musgrave, Crystal Acoustics, Holden Day, San Francisco, CA (1970).
- [2] G.F.D. Duff, "The Cauchy problem for elastic waves in an anisotropic medium", Philos. Trans. Roy. Soc. London A 252, 31-273 (1960).
- [3] E.A. Kraut, "Advances in the theory of anisotropic elastic wave propagation", Rev. Geophys. 1, 401-447 (1963).
- [4] R.G. Payton, Elastic Wave Propgation in Transversely Isotropic Media, Nijhoff, The Hague (1983).
- [5] A.N. Norris, B.S. White and J.R. Schrieffer, "Gaussian wave packets in inhomogeneous media with curved interfaces", Proc. Roy. Soc. London A 412, 93-123 (1987).
- [6] V. Cerveny and I. Psencik, "Gaussian beams and paraxial ray approximation in three-dimensional elastic inhomogeneous media", J. Geophys. 53, 1-15 (1983).
- [7] A.N. Norris, "Elastic Gaussian wave packets in isotropic media", Acta Mech. (1987), to appear.

- [8] V. Cerveny, I.A. Molotkov and I. Psencik, Ray Method in Seismology, University of Karlova, Prague (1977).
- [9] V. Cerveny, "Seismic rays and ray intensities in inhomogeneous anisotropic media", J. Geophys. 28, 1-13 (1972).
- [10] H. Murakami and G.A. Hegemier, "A mixture model for unidirectionally fiber-reinforced composites", J. Appl. Mech. 53, 765-773 (1986).
- [11] V.T. Buchwald, "Elastic Waves in Anisotropic Media", Proc. Roy. Soc. London A 253, 563-580 (1959).